Int J Radiat Biol. Author manuscript; available in PMC 2013 November 14.

Published in final edited form as:

Int J Radiat Biol. 2012 January ; 88(1-2): 15–21. doi:10.3109/09553002.2011.577505.

Measurement of inelastic cross sections for low-energy electron scattering from DNA bases

Marc Michaud[1], **Marc. Bazin**[1], and **Léon Sanche**[1,2]

[1]Department of Nuclear Medicine and Radiobiology

[2]Centre for Radiotherapy Research (CR[2])

Abstract

Purpose—Determine experimentally the absolute cross sections (CS) to deposit various amount of energies into DNA bases by low-energy electron (LEE) impact.

Materials and methods—Electron energy loss (EEL) spectra of DNA bases are recorded for different LEE impact energies on the molecules deposited at very low coverage on an inert argon (Ar) substrate. Following their normalisation to the effective incident electron current and molecular surface number density, the EEL spectra are then fitted with multiple Gaussian functions in order to delimit the various excitation energy regions. The CS to excite a molecule into its various excitation modes are finally obtained from computing the area under the corresponding Gaussians.

Results—The EEL spectra and *absolute* CS for the electronic excitations of pyrimidine and the DNA bases thymine, adenine, and cytosine by electron impacts below 18 eV are reported for the molecules deposited at about monolayer coverage on a solid Ar substrate.

Conclusions—The CS for electronic excitations of DNA bases by LEE impact are found to lie within the 10^{-16} – 10^{-18} cm^2 range. The large value of the total ionisation CS indicates that ionisation of DNA bases by LEE is an important dissipative process via which ionising radiation degrades and is absorbed in DNA.

Keywords

Electron energy loss; Cross sections; DNA bases; Electronic excitations

1. Introduction

The genotoxic effects of ionizing radiation in cells result from the transfer of the primary ionizing radiation energy to the production of a large number of secondary low-energy electrons (LEE) having energies below ~ 100 eV along with ion, radical, and excited species, which are created by both the primaries and these LEE. This chain of events can be

Marc Michaud, Université de Sherbrooke, Faculté de médecine et des sciences de la santé, 3001, 12e Avenue Nord, Sherbrooke (Québec), Canada J1H 5N4, Marc.Michaud@USherbrooke.ca.

Declaration of interest: The authors report no conflicts of interest. The authors alone are responsible for the content and writing of the paper.

described with detailed-history Monte Carlo (MC) simulations that account event-by-event for the slowing down of all generations of particles in matter and thus can provide a local dosimetry at the sub-cellular level and thus links directly the dose to the biological effects (Nikjoo et al. 2008, Zhang and Tan 2010). Several research groups have developed such MC codes to investigate the effects of charged particle track structure on the production of various DNA damage in a biomolecular target; for an extended review on transport codes see Nikjoo et al. (2006). Although considerable progress is being made in the incorporation of large biomolecular target into the MC codes, unfortunately the essential input, that is the cross section (CS) data for LEE interactions with important biomolecules particularly water and DNA are still lacking. The reason for this lies in the aggregation and condensed-phase effects along with the low-energy range where both experiments and theoretical calculations are difficult to perform (Tan et al. 2004; Emfietzoglou and Nikjoo 2005, Nikjoo et al. 2008).

In view of the large number LEE produced either by the passage of ionising radiation in cells or by short-range Auger electron emitters bound or incorporated into DNA of cells, what are (a) the CS for various energy deposits by LEE at sites H_2O, phosphate, sugar, adenine, thymine, cytosine, guanine, lysine, hystidine, arginine, … and (b) the probabilities to form new species (i.e., cations, anions, and radicals) from fast energy decay and bond rupture processes following the collisions in (a)? In an effort to provide a number of answers to these interrogations, several experimental studies have been carried out on electron impact on individual DNA bases to understand what fragments are generated. Most of them concern the formation of various anion fragments produced by dissociative electron attachment to these molecules in gas phase (Huels et al. 1998, Aflatooni et al. 1998, 2006, Abdoul-Carime et al. 2000, 2004, Abouaf et al. 2003, 2003b, Denifl et al. 2003, 2004a, 2004b, Ptasinska et al. 2005a, 2005b, Abouaf and Dunet 2005) and sublimated as thin films (Herve Du Penhoat et al. 2001, Abdoul-Carime et al. 2001). Few studies have also examined their electronic and vibrational excitations by electron-energy loss (EEL) spectroscopy in the gas phase (Dillon et al. 1989, Abouaf et al. 2003a, 2004). So far, not much attention has been devoted on the determination of the *absolute* CS for these different collision processes.

In line with these latter requirements, we present a short review of the quantitative studies of the interaction of LEE with DNA bases that have been undertook in our laboratory during the last decade. The EEL apparatus, sample preparation system, experimental method along with the scattering model to extract the CS are described. The EEL spectra and *absolute* CS for the electronic excitations of pyrimidine (Levesque et al. 2005b) and the DNA bases thymine (Levesque et al. 2003, 2005a, 2005c), adenine (Panajotovic et al. 2007) and cytosine (Bazin et al. 2010) by electron impacts below 20 eV are reported for the molecules deposited at very low coverage on a inert solid argon (Ar) substrate.

II. Scattering model and measurement methods

In our experiments an electron beam of current I_0 and energy E_0 provided by a monochromator, which has been described in details previously (Sanche and Michaud 1984), is incident at an angle θ_0 on a thin film of DNA molecules. The latter is prepared under ultra-high vacuum (UHV) condition with a double-stage oven system (Levesque et al. 2005c) by sublimation onto a solid spacer of Ar (Matheson, Whitby, ON, Canada)

condensed on a substrate of platinum (Pt) (Goodfellow, Oakdale, PA, USA) at a temperature of 18 K. The current of electron backscattered in the direction θ_d with an energy E is measured as a function of the energy transferred $E - E_0$ to the molecules by an analyser (Sanche and Michaud 1984). Under single collision and near normal incidence conditions, it can be shown (Levesque et al. 2005b) that the expression for such a current energy distribution also called EEL spectrum reduces to

$$I(\theta_d, E_0, E-E_0) \cong \frac{I_0(\theta_d, E_0)}{\cos\theta_0}\sigma_r(E_0, E-E_0)n_S. \quad (1)$$

Here $I_0(\theta_d, E_0)$ is an effective incident electron current, which may be seen as the portion of the incident current I_0 that would be backscattered into the analyser in the same direction θ_d by a model material having an elastic reflectivity equal to one. In practice, it is obtained from extrapolating the linear relationship found between the total reflected (i.e., energy integrated EEL spectrum) and transmitted currents as a function of increasing molecular coverage on the substrate. The quantity $\sigma_r(E_0, E - E_0)$ is a CS per unit energy transfer range for an electron of energy E_0 to deposit an energy $E - E_0$ on a single molecule and be backscattered over the whole half-angular space. The factor 1/cos θ_0 accounts for the projection of the incident electron beam section onto the film surface. Finally, n_S is the calibrated surface number density of molecules on the substrate. Given $I_0(\theta_d, E_0)$ along with n_S, $\sigma_r(E_0, E - E_0)$ is immediately obtained from an EEL spectrum using Equation 1. It is then fitted with multiple Gaussian functions to delimit the various excitation energy regions. Finally, the scattering CS to excite a molecule in its various excitation modes are obtained from the areas under the corresponding Gaussian distributions.

III. Results

The electronic EEL spectra of thin films of pyrimidine (Sigma-Aldrich, Oakville, ON, Canada), thymine (Sigma-Aldrich, Oakville, ON, Canada), adenine (Sigma-Aldrich, Oakville, ON, Canada), and cytosine (Sigma-Aldrich, Oakville, ON, Canada), which are sublimated onto the Ar substrate, are shown in Figure 1 in panels (a), (b), (c) and (d), respectively. All EEL spectra were recorded with the monochromator oriented near to the normal to the sample at $\theta_0 = 15°$ along with the analyser fixed at $\theta_d = 45°$. The vertical scales correspond to $\sigma_r(E_0, E - E_0)$ and have the dimension of area × energy $^{-1}$. The thin continuous lines passing through each of the spectra result from curve fitting with multiple Gaussian functions to delimit the various electronic excitation regions, as shown in the bottom of each of the panels.

Pyrimidine

Electronic EEL spectra of 3 layers of pyrimidine were recorded for several incident energies E_0 between 6 and 12 eV (Levesque et al. 2005b). The spectrum at $E_0 = 12$ eV along with the resulting Gaussians are shown in Figure 1(a). Sensitivity to symmetry- and spin-forbidden transitions as well as correlations to the triplet states of benzene (Sanche and Michaud 1981), made it possible to ascribe the main features, below 7 eV to triplet transitions. The

lowest EEL feature with an energy onset at 3.5 eV was attributed to a transition to the $^3B_1(n \rightarrow \pi^*)$ valence electronic state whereas the lack of minimum around 4.5 eV to the excitation of both the $^3A_2(n \rightarrow \pi^*)$ and $^1A_2(n \rightarrow \pi^*)$ states. The remaining EEL features at 4.3, 5.2, 5.8, and 6.5 eV were all assigned to $\pi \rightarrow \pi^*$ transitions to states of symmetry $^3A_1$, $^3B_2$ with $^3A_1$, $^3B_2$, and $^3B_2$ along with $^3A_1$, respectively. The most intense maximum at 7.6 eV was found to correspond to both $^1B_2$ and $^1A_1$ transitions, as in the vacuum ultraviolet (VUV) spectra (Bolovinos et al. 1984).

The electron scattering CS between 6 and 12 eV for the above electronic states are reported in Table I. The fixed energy positions and full width at half maximum (FWHM) of the Gaussians are specified in the caption to Table I. The Gaussian E_I stands for the $^3A_1$, $^3A_2$ and $^1A_2$ transitions, E_{II} for the $^3B_2$ and $^3A_1$ transitions, E_{III} for the $^3B_2$, $^3B_2$ and $^3A_1$ transitions, whereas the singlet excitations to the $^1B_2$ and $^1A_1$ states are combined under E_{IV}. The contribution included under the E_R label is the overall CS for the remaining EEL signal. For instance, at the incident energy of 12 eV, it essentially accounts for the EEL signal between 7.6 eV and 12 eV that is not included under the E_{IV} Gaussian.

Thymine

Electronic EEL spectra of 1.4 layers of thymine were recorded for several incident energies E_0 between 5 and 12 eV (Levesque et al. 2005a). The spectum at E_0 = 12 eV along with the resulting Gaussians are shown in Figure 1(b). The energies and relative magnitudes of the EEL features bear the closest resemblance to those observed for thymine in the gas phase (Abouaf et al. 2003a). Hence, the two lowest overlapping EEL features at 3.7 and 4 eV were ascribed to the excitation of the triplet $1^3A'(\pi_2 \rightarrow \pi_3^*)$ and $1^3A''(n_2 \rightarrow \pi_3^*)$ valence states of the molecule (Marian et al. 2002). The peak seen at 4.9 eV was ascribed to the excitations of the $2^3A'(\pi_1 \rightarrow \pi_3^*)$ state with a possible contribution from the $2^1A'(\pi_2 \rightarrow \pi_3^*)$ state. The weak shoulder around 6.0 eV was attributed to the excitation of both the $3^3A'(\pi_2 \rightarrow \pi_4^*)$ and $2^3A''$ $(n_2 \rightarrow \pi_4^*)$ states. The following maximum at 6.3 eV was found to arise from transitions to both $4^3A'(\pi_1 \rightarrow \pi_4^*)$ and $3^3A''$ $(n_1 \rightarrow \pi_3^*)$ states along with a possible contribution from the $3^1A'(\pi_1 \rightarrow \pi_3^*)$ state. The broad feature at 7.3 eV was attributed to the excitations of the $5^3A'(\pi_0 \rightarrow \pi_3^*)$ state along with the $5^1A'(\pi_1 \rightarrow \pi_4^*)$ state and the shallow band around 9 eV to the $6^1A'(\pi_0 \rightarrow \pi_3^*)$ state.

The CS to excite the above electronic states by electron impact between 5 and 12 eV are reported in Table II. The constant energy positions and FWHM of the Gaussians are also specified in the caption to Table II. The Gaussian E_I stands for both transitions to the $1^3A'$ and $1^3A''$ states, E_{II} to the $2^3A'$ and $2^1A'$ states, E_{III} to the $3^3A'$, $2^3A''$, $4^3A'$, $3^3A''$ states along with the $3^1A'$ state, whereas the excitation of the 5^3A and 5^1A states are taken as the distribution E_{IV}. The contribution included under the E_R label is the overall CS for the remaining EEL signal. For instance, at the incident energy of 12 eV, it essentially accounts for the EEL signal between 7.3 eV and 12 eV, which includes excitation of the $6^1A'$ state.

The CS obtained for thymine were found to be in general 1.5 times higher than those for pyrimidine. This difference in magnitude, although it falls well within the overall experimental uncertainties, could be traced back more particularly to the higher film thickness used in the case of pyrimidine (i.e., 3 layers). In fact for thymine, the EEL

intensities were measured to be directly proportional to the amount of deposited thymine up to about 1.4 layers. The departure from the linear behavior manifests as a monotonous signal drop of about 20% at 2.5 layers that tends progressively to a saturation level at higher coverages. This phenomenon is expected from the finite electron beam probing depth that stems from the total electron mean free path, and beyond which the molecules in a film can no longer be detected efficiently. Consequently, in the case of pyrimidine, having assumed that the EEL signal was linear with the coverage and thus having merely divided the EEL spectra by the 3-layer film coverage, suggests that those CS could be underestimated by 20 to 30%. In conclusion, if the thickness had been the same in both case (i.e., 1.4 layer), the CS would have been found more similar.

Adenine

The EEL spectra of a monolayer of adenine were recorded for several incident energies E_0 between 8 and 12 eV (Panajotovic et al. 2007). The spectrum at E_0 = 12 eV is shown in Figure 1(c). In this case, the energy position of the Gaussians were initially constrained to be in the range of energies in the theoretical studies (Mishra et al. 2000, Preuss et al. 2004, Sobolewski and Domcke 2002, Marian 2005) and measured in the experiments (Dillon et al. 1989, Mishra et al. 2000, Preuss et al. 2004, Isaacson 1972). The spectrum could so be deconvoluted into five Gaussians at the 4.7, 5.0, 5.5, 6.1, and 6.6 eV. Beyond the energy loss of 6.8 eV the spectrum was too broad and featureless and did not give us an indication where the possible excited states should be. In adenine, since the lowest triplet states predicted at 3.63 and 4.42 eV (Marian 2005) were not clearly visible in the spectra for E_0 above 8 eV, they were also not included in the analysis. Furthermore, the proximity of triplet and singlet states, which has been predicted above 4 eV by Marian (2005), did not allow us to distinguish between them in the EEL spectrum.

The electron scattering CS between 8 and 12 eV corresponding to the above electronic states E_{I}, E_{II}, E_{III}, E_{IV} and E_{V} are reported in Table III. The constant energy positions and FWHM of the Gaussians are also specified in the caption to Table III. The residual CS corresponding to E_{R} was calculated as the difference between the convoluted curve and the EEL spectrum and stands for the contribution from the electronic excitations beyond 6.8 eV. These CS were found to be in the same range from 10^{-18} to 10^{-17} cm^2 as those of thymine (Table II).

Cytosine

The electronic EEL spectra of a monolayer of cytosine were recorded for E_0 between 5 and 18 eV, a larger incident energy range than for the previous molecules (Bazin et al. 2010). A survey EEL spectrum, which results from averaging ten different scans between E_0 = 9 and 18 eV is shown along with the resulting Gaussian distributions in Figure 1(d). The dashed line accounts for the background contribution arising from multiple energy losses into the underlying substrate (Goulet et al. 1994). The sharp rise above 11.5 eV is due to electronic transitions in the Ar substrate (Michaud and Sanche 1994) and as such imposes an upper limit to the investigated EEL range. The energies and relative magnitudes of these EEL features were found to bear the closest resemblance to those observed by EEL spectroscopy of cytosine in the gas phase (Abouaf et al. 2004). In that work the first two features at 3.5 and 4.25 eV, which appear essentially at low impact energies and large scattering angles,

have been attributed to triplet states. Since the scattering conditions in Figure 1 were similar to those conditions, the two lowest features at 3.55 and 4.02 eV were assigned to the excitation of the $1^3A'(\pi \rightarrow \pi^*)$ and $2^3A'(\pi \rightarrow \pi^*)$ triplet valence states of the molecule. The peak seen at 4.65 eV was recognised as the transition from the ground state to the singlet $2^1A'(\pi \rightarrow \pi^*)$ state. The small peak at 5.01 eV was explained by the excitations of both the singlet $1^1A''$ $(n \rightarrow \pi^*)$ and triplet $1^3A''$ $(n \rightarrow \pi^*)$ states, which have been calculated at about the same energy and to be separated by only about 0.2 eV (Fleig et al. 2007). The following shoulder at 5.39 eV was assigned to the excitation of the singlet $3^1A'$ $(\pi \rightarrow \pi^*)$ state along with some contribution from the triplet $3^3A'(\pi \rightarrow \pi^*)$ state that has been predicted at 5.27 eV (Fleig et al. 2007). The maximum at 6.18 eV followed by the weak shoulder at 6.83 eV was attributed to the $4^1A'(\pi \rightarrow \pi^*)$ and $5^1A'(\pi \rightarrow \pi^*)$ singlet states, respectively, similarly to the gas phase. Finally, the broad band at 7.55 eV was found to arise from the singlet $6^1A'(\pi \rightarrow \pi^*)$ state, which has been located around 8 eV in the gas phase (Abouaf et al. 2004) and 7.35 eV in VUV spectroscopy of sublimed films (Raksanyi et al. 1978). The Gaussians labeled I_1, I_2, I_3, and I_4 at about 8.55, 9.21, 9.83, and 11.53 eV, respectively, were compared to valence shell photoelectron spectrum of cytosine in the gas phase (Trofimov et al. 2006). In that spectrum the vertical ionisation energies of the molecule in its ground state (i.e., binding energies) encompassing the four highest occupied molecular orbitals (MO) have been found at 8.89, 9.55, 9.89, and 11.64 eV along with a shallow shoulder at about 11.20 eV.

The CS to excite various electronic states of cytosine by electron impact at different E_0 are listed in Table IV. The constant energy positions and FWHM of the Gaussians are also specified in the caption to Table IV. In contrast to our previous works, the EEL spectra at different E_0 and so the impact energy dependences of the various CS were obtained for exactly the same cytosine coverage on the inert Ar substrate. The end result was an important reduction of the scatter suffered by the previous data and which was due to the use of a new molecular deposition for each of the incident energies. In general, the CS are found to be in the same range from 10^{-18} to 10^{-17} cm^2 as those of thymine (Table II). The sum of the CS attributed to the ionisation potential I_1, I_2, I_3, and I_4 (Table IV) rises steeply to a maximum of 8.1×10^{-16} cm^2 at the incident energy of 13 eV and then falls. This drop is due to the fact that the analysis was limited to an EEL energy of 12 eV and thus ignored the contribution from the inner valence shell MO, which have been found at about 12.93, 13.86, 14.94 and 18.02 eV in the gas phase (Trofimov et al. 2006). No experimental CS data for electron impact ionisation of cytosine have been published, but the total ionisation CS has been calculated for energies ranging from the ionisation threshold up to a few thousand eV by several groups using semi-classical and binary-encounter-Bethe formalisms (Bernhardt et al. 2003, Mozejko and Sanche 2003). The present total ionisation CS, which is linear the first few eVs above the ionisation threshold, is about three times larger than the calculated one. This was explained in part by the fact that in an EEL spectrum recorded for E_0 just above an ionisation threshold, it is impossible to distinguish between a scattered and an ejected electron. So, if the latter contributed to half of the ionisation EEL signal (i.e., both electrons having about the same energy) the measured CS would be twice too large. Nonetheless, the still large total ionisation CS confirms that ionisation of DNA basis by LEE

is an important dissipative process via which ionising radiation degrades and is absorbed in DNA.

IV. Discussion and conclusion

The present CS are akin to an electron backscattered angular distribution that would be integrated over the whole half-angular space. If scattering was isotropic, such CS would correspond to half of the integral CS. Owing to these conditions, the present electronic excitation CS reflect short-range interactions, which include static-exchange and correlation effects as well as capture of the incident electron by a molecule or electron resonance (Schulz 1973). Electron exchange allows for instance the transition from an initial singlet ground state to a final triplet excited state (Allan 1989). Electron correlation effects at long range are responsible for the induced polarisation interaction that arises from virtual excitation of optically allowed electronic transitions (i.e., associated with the dipole moment) of the molecule (Lane 1980). When the incident electron energy E_0 exceeds the corresponding transition energies, the electron then suffers inelastic collisions, which transfer and partition its energy among the various electronic excitations.

The downward trend of the CS for the dipole allowed transitions (i.e., singlet states) with E_0, which is better observed in the case of cytosine, can be related to the kinematics of the electron-molecule collision (Inokuti 1971). Under the current scattering angle of 120° (i.e., $\theta_0 = 15°$, $\theta_d = 45°$), the electron wave-vector transfer associated to an excitation of 5 eV, for instance, increases from 1.15 $Å^{-1}$ at threshold up to 3.5 $Å^{-1}$ at E_0 of 18 eV. The same wave-vector transfer range would be achieved if E_0 was set to 200 eV and the scattering angle was varied from 9 to 28°. Since the CS for dipole allowed transitions are strongly forward peaked at such incident energy and thus decrease with increasing scattering angle, suggests that the present CS for the singlet states should reach a maximum slightly above their energy thresholds and then decrease with E_0.

Effect of the environment more specifically the presence of water on the present CS for the DNA bases remains to be investigated experimentally in more details. Differences may stem from static (e.g., dipole) and correlation (e.g., polarisation) interactions with the surrounding medium, excitation transfers (i.e., excitons), and coherent scattering. When the electron kinetic energy compares in magnitude to the valence excitation energies, these effects are expected to influence elastic and inelastic collisions involving small and large momentum transfer and thus scattering in the forward and backward directions. So far, EEL spectroscopy at 12-eV incident energy of water in close contact with thymine has revealed that the CS for the electronic excitations of the $^{3,1}B_1$ dissociative states of H_2O, which lead to the production of OH radicals, was reduced by a factor of about three in the presence of thymine (Cho et al. 2004). This finding was found to concur with radiation-induced DNA damage, which indicates a considerable reduction of bond ruptures under dry DNA conditions (i.e., 2.5 water molecules per nucleotide) (La Vere et al. 1996).

Our CS are directly related to dose calculation in targeted radionuclide therapy, which uses carriers containing radionuclides that emit weak β particles and/or short-range Auger electrons (i.e., LEE). Although, the contribution of LEE with their nm ranges is not required

in the conventional dosimetry of fast primary particles in a macroscopic volume, such as an organ, the same is not true when considering dose and damage heterogeneities at the level of the cell nucleus, the chromosome, or the DNA (Terrissol 2004). This situation is met, for example, when radiation dose is delivered with the concomitant administration of radiosensitisers or high molecular weight (i.e., high-Z) atoms that incorporate into DNA of the cancer cells (e.g., bromouridine and cis-platin). Under these conditions, the nanoscopic dose and the evaluation of DNA damage could both be underestimated in conventional dosimetry owing to the neglect of LEE.

Acknowledgments

This research was financed by the Canadian Institutes of Health Research (FRN 37766).

References

Abdoul-Carime H, Cloutier P, Sanche L. Low-energy (5–40 eV) electron-stimulated desorption of anions from physisorbed DNA bases. Radiation Research. 2001; 155:625–633. [PubMed: 11260665]

Abdoul-Carime H, Gohlke S, Illenberger E. Site-specific dissociation of DNA bases by slow electrons at early stages of irradiation. Physical Review Letters. 2004; 92:168103/1–168103/4. [PubMed: 15169265]

Abdoul-Carime H, Huels MA, Bruning F, Illenberger E, Sanche L. Dissociative electron attachment to gas-phase 5-bromouracil. Journal of Chemical Physics. 2000; 113:2517–2521.

Abouaf R, Dunet H. Structures in dissociative electron attachment cross-sections in thymine, uracil and halouracils. European Physical Journal D. 2005; 35:405–410.

Abouaf R, Pommier J, Dunet H. Electronic and vibrational excitation in gas phase thymine and 5-bromouracil by electron impact. Chemical Physics Letters. 2003a; 381:486–494.

Abouaf R, Pommier J, Dunet H. Negative ions in thymine and 5-bromouracil produced by low energy electrons. International Journal of Mass Spectrometry. 2003b; 226:397–403.

Abouaf R, Pommier J, Dunet H, Quan P, Nam PC, Minh TN. The triplet state of cytosine and its derivatives: electron impact and quantum chemical study. Journal of Chemical Physics. 2004; 121:11668–11674. [PubMed: 15634133]

Aflatooni K, Gallup GA, Burrow PD. Electron attachment energies of the DNA bases. Journal of Physical Chemistry A. 1998; 102:6205–6207.

Aflatooni K, Scheer AM, Burrow PD. Total dissociative electron attachment cross sections for molecular constituents of DNA. Journal of Chemical Physics. 2006; 125:054301/1–054301/5. [PubMed: 16942207]

Allan M. Study of triplet states and short-lived negative ions by means of electron impact spectroscopy. Journal of Electron Spectroscopy and Related Phenomena. 1989; 48:219–351.

Bazin M, Michaud M, Sanche L. Absolute cross sections for electronic excitations of cytosine by low energy electron impact. Journal of Chemical Physics. 2010; 133:155104/1–155104/9. [PubMed: 20969430]

Bernhardt P, Friedland W, Jacob P, Paretzke HG. Modeling of ultrasoft X-ray induced DNA damage using structured higher order DNA targets. International Journal of Mass Spectrometry. 2003; 223–224:579–597.

Bolovinos A, Tsekeris P, Philis J, Pantos E, Andritsopoulos G. Absolute vacuum ultraviolet absorption spectra of some gaseous azabenzenes. Journal of Molecular Spectroscopy. 1984; 103:240–256.

Cho W, Michaud M, Sanche L. Vibrational and electronic excitations of H_2O on thymine films induced by low-energy electrons. Journal of Chemical Physics. 2004; 121:11289–11295. [PubMed: 15634084]

Denifl S, Ptasinska S, Cingel M, Matejcik S, Scheier P, Mark TD. Electron attachment to the DNA bases thymine and cytosine. Chemical Physics Letters. 2003; 377:74–80.

Denifl S, Ptasinska S, Hanel G, Gstir B, Scheier P, Probst M, Farizon B, Farizon M, Matejcik S, Illenberger E, Mark TD. Electron attachment to uracil, thymine and cytosine. Physica Scripta T. 2004a; 110:252–255.

Denifl S, Ptasinska S, Probst M, Hrusak J, Scheier P, Mark TD. Electron attachment to the gas-phase DNA bases cytosine and thymine. Journal of Physical Chemistry A. 2004b; 108:6562–6569.

Dillon MA, Tanaka H, Spence D. The electronic spectrum of adenine by electron impact methods. Radiation Research. 1989; 117:1–7. [PubMed: 2913604]

Emfietzoglou D, Nikjoo H. The effect of model approximations on single-collision distributions of low-energy electrons in liquid water. Radiation Research. 2005; 163:98–111. [PubMed: 15606313]

Fleig T, Knecht S, Hattig C. Quantum-chemical investigation of the structures and electronic spectra of the nucleic acid bases at the coupled cluster CC2 level. Journal of Physical Chemistry A. 2007; 111:5482–5491.

Goulet T, Jung JM, Michaud M, Jay-Gerin JP, Sanche L. Conduction-band density of states in solid argon revealed by low-energy-electron backscattering from thin films: role of the electron mean free path. Physical Review B. 1994; 50:5101–5109.

Herve Du Penhoat MA, Huels MA, Cloutier P, Jay-Gerin JP, Sanche L. Electron stimulated desorption of H^- from thin films of thymine and uracil. Journal of Chemical Physics. 2001; 114:5755–5764.

Huels MA, Hahndorf I, Illenberger E, Sanche L. Resonant dissociation of DNA bases by subionization electrons. Journal of Chemical Physics. 1998; 108:1309–1312.

Inokuti M. Inelastic collisions of fast charged particles with atoms and molecules-the Bethe theory revisited. Reviews of Modern Physics. 1971; 43:297–347.

Isaacson M. Interaction of 25 keV electrons with the nucleic acid bases, adenine, thymine, and uracil. I. Outer shell excitation. Journal of Chemical Physics. 1972; 56:1803–1812.

La Vere L, Becker D, Sevilla MD. Yields of $^{\bullet}$OH in gamma irradiated DNA as a function of DNA hydration: Hole transfer in competition $^{\bullet}$OH formation. Radiation Research. 1996; 145:673–680. (1996). [PubMed: 8643826]

Levesque PL, Michaud M, Cho W, Sanche L. Absolute electronic excitation cross sections for low-energy electron (5–12 eV) scattering from condensed thymine. Journal of Chemical Physics. 2005a; 122:224704/1–224704/7. [PubMed: 15974700]

Levesque PL, Michaud M, Sanche L. Absolute vibrational and electronic cross sections for low-energy electron (2–12 eV) scattering from condensed pyrimidine. Journal of Chemical Physics. 2005b; 122:94701/1–94701/10.

Levesque PL, Michaud M, Sanche L. Cross sections for low energy (1–12 eV) inelastic electron scattering from condensed thymine. Nuclear Instruments and Methods in Physics Research B. 2003; 208:225–230.

Levesque PL, Michaud M, Sanche L. Double sublimation system to deposit molecules from solid organic compounds onto a cryogenic substrate: thymine on solid argon. Review of Scientific Instruments. 2005c; 76:103901/1–103901/6.

Marian CM. A new pathway for the rapid decay of electronically excited adenine. Journal of Chemical Physics. 2005; 122:104314/1–104314/13. [PubMed: 15836322]

Marian CM, Schneider F, Kleinschmidt M, Tatchen J. Electronic excitation and singlet-triplet coupling in uracil tautomers and uracil-water complexes. A quantum chemical investigation. European Physical Journal D. 2002; 20:357–367.

Michaud M, Sanche L. Low-energy electron-energy-loss spectroscopy of solid films of argon: surface and bulk valence excitons. Physical Review B. 1994; 50:4725–4732.

Mishra SK, Shukla MK, Mishra PC. Electronic spectra of adenine and 2-aminopurine: an ab initio study of energy level diagrams of different tautomers in gas phase and aqueous solution. Spectrochimica Acta. 2000; 56A:1355–1384. [PubMed: 10888441]

Mozejko P, Sanche L. Cross section calculations for electron scattering from DNA and RNA bases. Radiation and Environmental Biophysics. 2003; 42:201–211. [PubMed: 14523567]

Nikjoo H, Emfietzoglou D, Watanabe R, Uehara S. Can Monte Carlo track structure codes reveal reaction mechanism in DNA damage and improve radiation therapy? Radiation Physics and Chemistry. 2008; 77:1270–1279.

Nikjoo H, Uehara S, Emfietzoglou D, Cucinotta FA. Track-structure codes in radiation research. Radiation. Measurements. 2006; 41:1052–1074.

Panajotovic R, Michaud M, Sanche L. Cross sections for low-energy electron scattering from adenine in the condensed phase. Physical Chemistry Chemical Physics. 2007; 9:138–148. [PubMed: 17164896]

Preuss M, Schmidt WG, Seino K, Furthmuller J, Bechstedt F. Ground- and excited-state properties of DNA base molecules from plane-wave calculations using ultrasoft pseudopotentials. Journal of Computational Chemistry. 2004; 25:112–122. [PubMed: 14634999]

Ptasinska S, Denifl S, Grill V, Mark TD, Illenberger E, Scheier P. Bond- and site-selective loss of H− from pyrimidine bases. Physical Review Letters. 2005a; 95:093201/1–093201/4. [PubMed: 16197213]

Ptasinska S, Denifl S, Grill V, Mark TD, Scheier P, Gohlke S, Huels MA, Illenberger E. Bond-selective H− ion abstraction from thymine. Angewandte Chemie - International Edition. 2005b; 44:1647–1650. [PubMed: 15704232]

Raksanyi K, Foldvary I, Fidy L, Kittler L. The Electronic Structure of Cytosine, Lj-Azacytosine, and 6-Azacytosine. Biopolymers. 1978; 17:887–896.

Sanche L, Michaud M. Interaction of low-energy electron (1 – 30 eV) with condensed molecules: II. Vibrational-librational excitation and shape resonances in thin N_2 and CO films. Physical Review B. 1984; 30:6078–6092.

Sanche L, Michaud M. Electron energy-loss vibronic spectroscopy of matrix-isolated benzene and multilayer benzene films. Chemical Physics Letters. 1981; 80:184–187.

Schulz GJ. Resonances in electron impact on diatomic molecules. Reviews of Modern Physics. 1973; 45:423–486.

Sobolewski AL, Domcke W. On the mechanism of nonradiative decay of DNA bases: ab initio and TDDFT results for the excited states of 9H-adenine. European Physical Journal D. 2002; 20:369–374.

Tan Z, Xia Y, Liu X, Zhao M, Ji Y, Li F, Huang B. Cross sections of electron inelastic interactions in DNA. Radiation and Environmental Biophysics. 2004; 43:173–182. [PubMed: 15526117]

Terrisol M, Edel S, Pomplun E. Computer evaluation of direct and indirect damage induced by free and DNA-bound Iodine-125 in the chromatin fibre. International Journal of Radiation Biology. 2004; 80:905–908. [PubMed: 15764400]

Trofimov AB, Schirmer J, Kobychev VB, Potts AW, Holland DMP, Karlsson L. Photoelectron spectra of the nucleobases cytosine, thymine and adenine. Journal of Physics B. 2006; 39:305–329.

Zhang L, Tan Z. A new calculation on spectrum of direct DNA damage induced by low-energy electrons. Radiation and Environmental Biophysics. 2010; 49:15–26. [PubMed: 20039050]

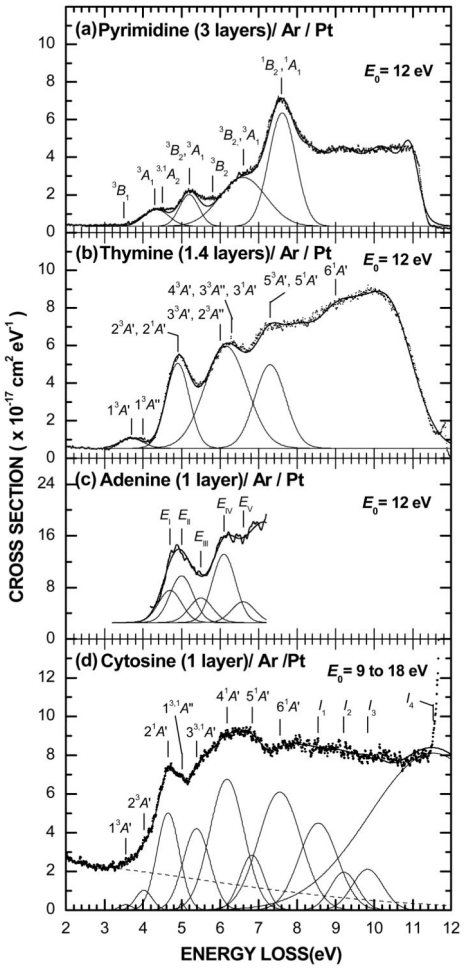

Figure 1.

(a) Electronic EEL spectrum at the incident electron energy E_0 = 12 eV of 3 layers of pyrimidine deposited on a 6-layer spacer of Ar condensed on the Pt substrate. (b) Electronic EEL spectra at E_0 = 12 eV of 1.4 layers of thymine deposited on a 6-layer spacer of Ar. (c) Electronic EEL spectrum at E_0 = 12 eV of a monolayer of adenine deposited on a 6-layer spacer of Ar. (d) Survey electronic EEL spectrum of monolayer of cytosine deposited on a 3-layer spacer of Ar. The thin solid line passing through each of the spectra results from curve fitting with multiple Gaussian functions delimiting the different electronic excitation regions, as shown in the bottom of each panel. The dashed line accounts simply for the background contribution arising from multiple energy losses in the Ar/Pt substrate.

Table I

Cross sections σ_{ii} (10^{-17} cm^2) for electronic excitations of pyrimidine by electron impact at different energies E_0 (eV).

	Electronic states				
E_0	E_I ($^3A_1$, $^3A_2$, $^1A_2$)	E_{II} ($^3B_2$, $^3A_1$)	E_{III} ($^3B_2$, $^3B_2$, $^3A_1$)	E_{IV} ($^1B_2$, $^1A_1$)	E_R
6	3.1				1.3
8	4.8	6.6			9.9
10	2.5	3.5	11.0		6.6
12	0.82	1.2	3.8	6.0	12.9

Gaussian distributions: E_I at 4.3(0.65) eV; E_{II} at 5.2(0.5) eV; E_{III} at 6.6(1.2) eV; E_{IV} at 7.6(0.7) eV; E_R remaining electronic cross section. The values within parentheses are the FWHM of the Gaussians

Table II

Cross sections σ_{fi} (10^{-17} cm^2) for electronic excitations of thymine by electron impact at different energies E_0 (eV).

	Electronic states				
E_0	E_{I} ($1\,^3A'$, $1^3A''$)	E_{II} ($2\,^3A'$, $2^1A'$)	E_{III} ($3\,^3A'$, $2^3A''$, $4^3A'$, $3^3A''$, $3^1A'$)	E_{IV} ($5\,^3A'$, $5^1A'$)	E_{R}
5	2.9	0.9			
6	1.6	5.3	0.7		
7	1.6	6.3	7.0		
8	1.8	6.8	13.6	2.2	
9	1.4	6.9	12.3	3.1	6.4
10	1.0	5.7	11.5	3.1	13.5
11	0.8	5.0	8.5	3.0	22.1
12	0.3	3.5	6.6	4.5	29.8

Gaussians distributions: E_{I} at 3.7(0.6) eV; E_{II} at 4.9 eV(0.6) eV; E_{III} at 6.1(1.1) eV; E_{IV} at 7.3(0.8) eV; E_{R} remaining electronic cross section. The values within parentheses are the FWHM of the Gaussians.

Table III

Cross sections σ_{ii} (10^{-17} cm^2) for electronic excitations of adenine by electron impact at different energies E_0 (eV).

	Electronic states					
E_o	E_I	E_{II}	E_{III}	E_{IV}	E_V	E_R
8	4.3	8.8	7.3	10.6	4.1	0.04
9	4.4	5.4	4.2	8.4	5.0	3.4
10	3.9	6.9	5.1	8.3	7.3	4.5
11	3.6	4.1	3.6	7.7	6.3	3.4
11.5	4.2	5.9	3.7	9.3	8.3	4.7
12	3.8	5.5	3.5	7.7	3.2	5.0

Gaussian distributions: E_I at 4.7(0.7) eV; E_{II} at 5(0.7) eV; E_{III} at 5.5(0.7) eV; E_{IV} at 6.1(0.7) eV; E_V at 6.6(0.7) eV; E_R remaining electronic cross sections. The values within parentheses are the FWHM of the Gaussians.

Table IV

Cross sections σ_{ri} (10^{-17} cm^2) for electronic excitations of cytosine by electron impact at different energies E_0(eV).

	Electronic states											
E_0	$1\,^3A'$	$2\,^3A'$	$2\,^1A'$	$1\,^1A''$	$3\,^1A'$	$4\,^1A'$	$5\,^1A'$	$6\,^1A'$	I_1	I_2	I_3	I_4
5	0.76	3.62	1.42									
6	1.84	4.94	10.36	0.15	5.33							
7	0.89	2.85	10.42	0.38	12.65	7.33						
8	0.67	1.65	8.08	0.31	9.48	17.87	6.47	1.08				
9	0.45	1.39	7.20	0.11	7.37	14.31	4.81	14.56	1.70			
10	0.35	0.98	6.10	0.23	6.88	12.31	3.23	16.37	10.31	4.30		
11	0.24	0.58	4.92	0.06	5.23	11.70	2.85	12.62	12.86	6.05	8.24	3.05
12	0.14	0.62	4.24	0.12	4.16	9.24	3.15	11.26	10.71	5.25	10.18	18.69
13	0.19	0.58	3.80	0.05	3.51	7.75	2.34	9.08	6.73	1.41	1.85	71.09
14	0.16	0.48	3.08	0.06	2.91	6.06	1.67	6.95	5.22	1.85	1.57	58.95
15	0.07	0.46	2.52	0	2.10	4.81	1.32	4.99	3.98	1.11	1.34	47.39
16	0.01	0.40	2.14	0.01	1.87	3.84	1.06	3.91	2.87	0.90	0.60	36.72
17	0.02	0.32	1.79	0	1.70	3.36	0.89	3.35	2.35	0.84	0.42	27.36
18	0	0.30	1.56	0	1.62	2.96	0.97	3.04	2.10	0.61	0.67	21.98

Gaussian distributions: $1^3A'$ at 3.55(0.37) eV, $1^3A'$ at 4.02(0.51) eV, 2^1A at 4.65(0.68) eV, $1^1A''$ at 5.01(0.15) eV, $3^1A'$ at 5.39(0.81) eV, $4^1A'$ at 6.18(1.04) eV, $5^1A'$ at 6.83(0.73) eV, $6\,^1A'$ at 7.55(1.30) eV, I_1 at 8.55(1.18) eV, I_2, at 9.21(0.83) eV, I_3 at 9.83(0.93) eV, and I_4 at 11.53(3.91) eV. The values within parentheses are the FWHM of the Gaussians.